PHY Layer Abstraction for SU-MIMO LTE System Employing Parallel Interference-Aware Detection

Elena Lukashova, Florian Kaltenberger, Raymond Knopp, Christian Bonnet

EURECOM

Campus SophiaTech, 450 Route des Chappes,

06410 Biot, France

Email: (elena.lukashova@eurecom.fr)

Abstract—**Maximum-likelihood (ML) receivers are optimum receivers for MIMO systems, but their complexity grows exponentially with the modulation order of the codeword and the number of spatial layers. The Reduced Complexity ML (R-ML) receivers based on low complexity adaptation of the max-log MAP detector and reduction of searching space are a good compromise to satisfy complexity-performance trade-off. In this paper we investigate physical layer abstraction for single-user MIMO system with a R-ML receiver performing Parallel Interference Aware (PIA) detection. We develop a light-weight extended Mutual Information Effective SINR Mapping (MIESM) methodology based on look-up tables (LUT), which take the special non-linear nature of the PIA receiver into account. The results show that the proposed LUT-based MIESM abstraction method is as accurate as the direct MIESM abstraction, but at the same time has significantly less computational complexity. It can thus be easily used in performance prediction devices as well as system level simulators.**

I. INTRODUCTION

Deploying multiple antennas at the transmitter and receiver side, widely known as multiple-input multiple-output (MIMO), is a key technique to increase throughput in wireless communication systems. Based on the serving target, MIMO systems fall into Single-User MIMO (SU-MIMO) and Multi-User MIMO (MU-MIMO). Focused on serving one user, SU-MIMO aims to maximize system throughput by sending independent information streams on parallel spatial layers or increase reliability by transmitting the same data stream over multiple antennas, while MU-MIMO targets simultaneous scheduling of several users on the same time-frequency resource.

Maximum-likelihood (ML) receivers are optimum receivers for MIMO systems thanks to outstanding performance, but their complexity grows exponentially with the modulation order of the codeword (CW) and the number of spatial layers. On the other hand, linear receivers such as Zero-Forcing and Minimum Mean Square Error (MMSE) are easier to implement, but do not provide adequate levels of performance. This motivates the research community to look for a complexity-performance trade-off; one of the promising solutions is Reduced Complexity ML (R-ML) receiver which is based on low complexity adaptation of the max-log MAP detector and reduction of searching space. If the interfering CW is of a known QAM constellation, R-ML receiver can also benefit from interference awareness (IA).

PHY abstraction is a powerful tool for system performance evaluation which can be used in link level simulations as well as in real time measurements and forms a part of the User Equipment (UE) and eNodeB emulators in radio network performance prediction devices. With the traditional LTE simulators, the full set of the PHY procedures such as coding, modulation, convolution, demodulation and decoding consumes more than 80% of simulation time [1], and is not affordable in terms of time and CPU; the use of PHY abstraction reduces computational time by a factor of 100 [2]. The second PHY abstraction application is Link Adaptation: depending on the ill- or well-conditioned channel, the UE decides on the Channel Quality Indicator (CQI) to satisfy target Block Error Rate (BLER) under current channel conditions. The two most studied PHY abstraction approaches are Exponential Effective SINR Mapping (EESM) [3], which is widely used for linear receivers, and Mutual Information Effective SINR Mapping (MIESM) [4], [5], [6], which reflects the nature of the ML-family of receivers. Both methods estimate post-processed Link Quality Metric (LQM) such as Signal-to-Interference-plus-Noise Ratio (SINR) or Mutual Information (MI) per subcarrier and then compress the obtained array of elements into a single effective value per channel realization. MIESM approach is proven to outperform EESM [7], but has a drawback in terms of computation complexity. Moreover, the EESM approach is a weak choice in the presence of non-Gaussian interference [8] [9], since interference is, in this case, absorbed into Gaussian noise. While post-processed SINR computation is straightforward for linear receivers, it remains a challenging point for non-linear ones, where joint detection is performed over all spatial layers. In [10], the authors proposed to estimate post-processed SINR of a ML receiver by upper- and lower-bounding it with Signal-to-Noise-Ratio (SNR) of respectively Interference-free (IF) and MMSE receivers and applying calibration coefficients. This approach was then extended to R-ML IA case in [11], where adjusting coefficient also depends on the interference strength. Another approach to estimate post-processed SINR for ML receiver through polynomial approximation was presented in [5], but not well adapted to MIMO and does not consider the interference-aware case. PHY abstraction for MIMO ML-receivers was developed in [12] based on QR and QL factorization of the channel matrix. The authors upper and lower bound the performance of each of the streams and then use the average value in order

to characterize the achievable performance. In [9], to avoid time consuming on-line mapping between channel gains and MI, the authors store channel statistics and corresponding MI values in a LUT for a MU-MIMO system with R-ML IA receiver.

In this paper, we present and validate a light-weight PHY abstraction methodology for Physical Downlink Shared Channel (PDSCH) of the SU-MIMO system employing a R-ML IA receiver with Parallel IA (PIA) detection. Our methodology is based on precomputed 3D LUTs with MI for different constellation alphabets (QPSK, 16QAM and 64QAM) and is symmetrical if the modulations orders of the CWs are exchanged: instead of 9 LUT for all the possible combinations of MCS, it is sufficient to use only 6. The LUT quantization analysis is performed, and abstraction results with LUT are compared with the ones obtained from direct precise computations of MI.

The reminder is organized as follows: in Section II we describe the signal model and sub-optimal precoder selection strategy for Spatial Multiplexing in the 2×2 SU-MIMO system. Section III gives an overview and a comparative information theoretic analysis of non-linear receivers and detection mechanisms for Spatial Multiplexing. In Section IV we present the abstraction methodology for R-ML PIA receiver, while Section V validates the proposed methodology. Finally, we complete the paper with the conclusion in Section VI.

II. SYSTEM MODEL

A. Signal model

SU-MIMO closed loop spatial multiplexing also known as downlink transmission mode 4 (TM4) was introduced in LTE Release 8 and is designed to increase the system throughput by sending two CWs, dedicated to the same UE, over two or four spatial layers. An essential part of TM4 is channel state information (CSI) feedback: the UE estimates the channel matrix based on Reference Symbols (RS), computes the CQI, Precoder Matrix Indicator (PMI) and Rank Indicator (RI) to ensure a BLER not higher than 10% and feeds back the selected parameters to the eNodeB. We consider a scenario where an eNodeB equipped with $n_{\text{tx}} = 2$ transmit antennas sends two spatially multiplexed CWs (CW_0 and CW_1), with MCS^0 and MCS^1 respectively, to a UE with $n_{\text{rx}} = 2$ receive antennas. The received signal vector $\mathbf{y}_k \in \mathbf{C}^{2 \times 1}$ for the k-th subcarrier seen by the UE is given by

$$\mathbf{y}_k = \mathbf{H}_k \mathbf{P}_k \mathbf{x}_k + \mathbf{n}_k, \quad k = 1, 2..., K, \tag{1}$$

where $\mathbf{x}_k \in Q^{M_0, M_1}$ is the vector of two complex symbols x_0 and x_1 with variance of σ_0^2 and σ_1^2, $Q^{M_0, M_1} := Q^{M_0} \times Q^{M_1}$ is a cartesian product of two modulation alphabets Q^{M_0} and Q^{M_1}, $M_0, M_1 \in \{2, 4, 6\}$ are the modulation orders of the constellations, and $\mathbf{n}_k$ is a vector of Zero Mean Circularly Symmetric Complex Gaussian (ZMCSCG) white noise of double-sided power spectral density $N_0/2$ at the 2 receive antennas of UE. $\mathbf{H}_k = [\mathbf{h}_{0,k} \ \mathbf{h}_{1,k}]$ is 2×2 MIMO flat fading Rayleigh channel constructed from i.i.d. ZMCSCG random variables with a variance of 0.5 per dimension, while $\mathbf{P}$ is a

2×2 precoding matrix employed by the eNodeB at the k-th RE. For the sake of simplicity, we drop the subcarrier index for a moment and replace multiplication of the $\mathbf{H}$ and $\mathbf{P}$ with the effective channel $\mathbf{H}_{\text{eff}}$:

$$\mathbf{y} = \mathbf{H}_{\text{eff}} \mathbf{x} + \mathbf{n}, \tag{2}$$

where $\mathbf{H}_{\text{eff}} = [\mathbf{h}_{\text{eff0}} \ \mathbf{h}_{\text{eff1}}]$.

B. Suboptimal Precoder Selection Strategy

The precoder codebook $\mathbf{P}$ for TM4 is standardized by 3GPP and follows the equal gain transmission (EGT) principle with the possibility of swapping columns over the entire band:

$$\mathbf{P} \in \left\{ \frac{1}{\sqrt{4}} \begin{bmatrix} 1 & 1 \\ 1 & -1 \end{bmatrix}, \frac{1}{\sqrt{4}} \begin{bmatrix} 1 & 1 \\ j & -j \end{bmatrix} \right\}. \tag{3}$$

The criteria, based on which the UE makes a decision on a particular PMI to report, is a subject for a discussion. There are a few metric-based criteria to select a precoder matrix: maximum system throughput or maximum SINR at the receiver. For the first case, an exhaustive search over all possible received signal vector needs to be performed for both precoder matrices on a per-subband basis, which, being optimal, involves huge computational complexity of constrained MI, especially for high modulation orders. As a result, we propose in this work a precoder selection that maximizes MI for the first CW only. The UE selects the precoder matrix $\mathbf{P}$ which ensures that the effective channel of the first stream is stronger than the one of the second stream:

$$\left(\frac{\|\mathbf{h}_0 + \mathbf{h}_1\|^2}{\|\mathbf{h}_0 - \mathbf{h}_1\|^2}, \frac{\|\mathbf{h}_0 + j\mathbf{h}_1\|^2}{\|\mathbf{h}_0 - j\mathbf{h}_1\|^2} \right). \tag{4}$$

The choice between these two ratios can be performed by evaluating the correlation coefficient ρ_{10}:

$$\rho_{10} = \mathbf{h}_{\text{eff1}}^H \ \mathbf{h}_{\text{eff0}}. \tag{5}$$

Comparing real and imaginary parts of ρ_{10} on a per-subband basis, the UE picks up one $\mathbf{P}$ from the two options:

$$\mathbf{P} = \begin{cases} \frac{1}{\sqrt{4}} \begin{bmatrix} 1 & 1 \\ 1 & -1 \end{bmatrix}, & \begin{array}{l} \text{for } \Re(\rho_{10}) \geq \Im(\rho_{10}) \text{ and } \Re(\rho_{10}) \geq -\Im(\rho_{10}) \\ \text{or } \Re(\rho_{10}) \geq \Im(\rho_{10}) \text{ and } \Re(\rho_{10}) \leq -\Im(\rho_{10}) \end{array} \\ \\ \frac{1}{\sqrt{4}} \begin{bmatrix} 1 & 1 \\ j & -j \end{bmatrix}, & \begin{array}{l} \text{for } \Re(\rho_{10}) \leq \Im(\rho_{10}) \text{ and } \Re(\rho_{10}) \geq -\Im(\rho_{10}) \\ \text{or } \Re(\rho_{10}) \leq \Im(\rho_{10}) \text{ and } \Re(\rho_{10}) \leq -\Im(\rho_{10}) \end{array} \end{cases} \tag{6}$$

III. RECEIVER ARCHITECTURE AND DETECTION MECHANISMS

A. Reduced Complexity Maximum Likelihood Interference Aware Receiver for 2×2 MIMO

Over the last few years, enhancing system performance through advanced receiver architectures has been attracting more and more attention [13]. Trying to overcome the traditional drawback of the ML receiver – extremely high computational complexity, that exponentially grows with the number of spatial layers and modulation order, – the research community has mainly focused on the sub-optimal R-ML receiver design.

$$I\left(X_0, X_1; \mathbf{Y}|\mathbf{H}, \mathbf{P}, M_0, M_1\right) = \log(M_0 M_1) - \frac{1}{M_0 M_1 N_n} \left(\sum_{\mathbf{x} \in Q^{M_0, M_1}} \sum_{z}^{N_n} \log \sum_{\mathbf{x}' \in Q^{M_0, M_1}} \exp \left[\frac{-\|\mathbf{y} - \mathbf{HPx}'\|^2 + \|\mathbf{n}\|^2}{N_0} \right] \right) \quad (11)$$

$$I\left(X_0; \mathbf{Y}_{\mathrm{MF}}|\boldsymbol{\alpha}, \boldsymbol{\gamma}, M_0, M_1\right) = \log M_0 - \frac{1}{M_0 M_1 N_n} \left(\sum_{x_0 \in Q^{M_0}} \sum_{x_1 \in Q^{M_1}} \sum_{z}^{N_n} \log \frac{\sum_{x_0' \in Q^{M_0}} \sum_{x_1' \in Q^{M_1}} \exp[-\frac{1}{N_0}\|\mathbf{y}_{\mathrm{MF}} - \boldsymbol{\alpha}x_0' - \boldsymbol{\gamma}x_1'\|^2]}{\sum_{x_1'' \in Q^{M_1}} \exp[-\frac{1}{N_0}\|\mathbf{y}_{\mathrm{MF}} - \boldsymbol{\alpha}x_0 - \boldsymbol{\gamma}x_1''\|^2]} \right) \quad (12)$$

$$I_{\mathrm{IF}} > \underbrace{I\left(X_0, X_1; \mathbf{Y}|\mathbf{H}, \mathbf{P}, M_0, M_1\right)}_{I_{\mathrm{ML}}} = \underbrace{I\left(X_0; \mathbf{Y}|\mathbf{H}, \mathbf{P}, M_0, M_1\right) + I\left(X_1; \mathbf{Y}|X_0, \mathbf{H}, \mathbf{P}, M_0, M_1\right)}_{I_{\mathrm{SIC\text{-}IA}}}$$
$$> \underbrace{I\left(X_0; \mathbf{Y}_{\mathrm{MF}}|\boldsymbol{\alpha}, \boldsymbol{\beta}, M_0, M_1\right) + I\left(X_1; \mathbf{Y}_{\mathrm{MF}}|\boldsymbol{\alpha}, \boldsymbol{\gamma}, M_0, M_1\right)}_{I_{\mathrm{PIA}}} > I_{\mathrm{MMSE}} \quad (13)$$

In [14], the authors show that the soft decision bit metrics for the ML decoder can be simplified to the minimum distance between the received symbol and $\sqrt{M}/2$ constellation points on the real line. Matched filter (MF)- based R-ML detector, proposed in [15], reduces one complex dimension of the system without introducing a loss in performance thanks to the decoupling of the real and imaginary parts of the metric. SU-MIMO design can be seen as a system with two CWs that interfere with each other, which raises the question how the receiver should treat this interference. In classical non-IA receivers interference brings down the performance due to decreasing SINR. If interference is treated properly, the system is sensitive not to SINR, but to SNR [16]. Thus, if the ML receiver makes use of the discrete nature of interference, the system becomes noise-limited instead of being interference-limited. Closed-loop spatial multiplexing utilizes Downlink Control Information (DCI) format 2 that carries information about MCSs associated with the two transmitted Transport Blocks (TBs), thus, the SU-MIMO receiver can benefit from IA detection as well.

SU-MIMO multi-stream interference aware detection falls into three groups: ML, R-ML PIA and R-ML SIC-IA. Using the ML approach, the receiver performs decoding of the full transmitted vector simultaneously, while, in the R-ML PIA case, the decoder relies on soft-bit metrics obtained after performing maximum ratio combining (MRC) of the two compensated spatial layers. MFs $\frac{\mathbf{h}_{0\mathrm{eff}}^H}{\|\mathbf{h}_{0\mathrm{eff}}\|}$ and $\frac{\mathbf{h}_{1\mathrm{eff}}^H}{\|\mathbf{h}_{1\mathrm{eff}}\|}$ transform the cross-coupled MIMO channel in (2) into two compensated MISO channels with interference:

$$\mathbf{y}_{\mathrm{MF}} = \begin{bmatrix} y_{0\mathrm{MF}} \\ y_{1\mathrm{MF}} \end{bmatrix} = \begin{bmatrix} \frac{\mathbf{h}_{0\mathrm{eff}}^H \mathbf{h}_{0\mathrm{eff}}}{\|\mathbf{h}_{0\mathrm{eff}}\|} x_0 + \frac{\mathbf{h}_{0\mathrm{eff}}^H \mathbf{h}_{1\mathrm{eff}}}{\|\mathbf{h}_{0\mathrm{eff}}\|} x_1 + \frac{\mathbf{h}_{0\mathrm{eff}}^H}{\|\mathbf{h}_{0\mathrm{eff}}\|}\mathbf{n} \\ \frac{\mathbf{h}_{1\mathrm{eff}}^H \mathbf{h}_{0\mathrm{eff}}}{\|\mathbf{h}_{1\mathrm{eff}}\|} x_0 + \frac{\mathbf{h}_{1\mathrm{eff}}^H \mathbf{h}_{1\mathrm{eff}}}{\|\mathbf{h}_{1\mathrm{eff}}\|} x_1 + \frac{\mathbf{h}_{1\mathrm{eff}}^H}{\|\mathbf{h}_{1\mathrm{eff}}\|}\mathbf{n} \end{bmatrix}. \quad (7)$$

Note that MF, being a linear operation, does not change the noise variance. From the compensated received signal $\mathbf{y}_{\mathrm{MF}}$ the receiver detects symbol x_0 belonging to the first CW treating x_1 as interference, while the x_1 is obtained from the detection of $\mathbf{y}_{MF}$, where x_0 is considered as interference. For future reference we define the effective compensated channels and the received vector after MF:

$$\boldsymbol{\alpha} = \begin{bmatrix} \alpha_0 & \alpha_1 \end{bmatrix}^T = \begin{bmatrix} \frac{\mathbf{h}_{0\mathrm{eff}}^H \mathbf{h}_{0\mathrm{eff}}}{\|\mathbf{h}_{0\mathrm{eff}}\|} & \frac{\mathbf{h}_{1\mathrm{eff}}^H \mathbf{h}_{0\mathrm{eff}}}{\|\mathbf{h}_{1\mathrm{eff}}\|} \end{bmatrix}^T, \quad (8)$$

$$\boldsymbol{\gamma} = \begin{bmatrix} \gamma_0 & \gamma_1 \end{bmatrix}^T = \begin{bmatrix} \frac{\mathbf{h}_{0\mathrm{eff}}^H \mathbf{h}_{1\mathrm{eff}}}{\|\mathbf{h}_{0\mathrm{eff}}\|} & \frac{\mathbf{h}_{1\mathrm{eff}}^H \mathbf{h}_{1\mathrm{eff}}}{\|\mathbf{h}_{1\mathrm{eff}}\|} \end{bmatrix}^T, \quad (9)$$

$$\mathbf{y}_{\mathrm{MF}} = \boldsymbol{\alpha}x_0 + \boldsymbol{\gamma}x_1 + \begin{bmatrix} \frac{\mathbf{h}_{0\mathrm{eff}}^H}{\|\mathbf{h}_{0\mathrm{eff}}\|} & \frac{\mathbf{h}_{1\mathrm{eff}}^H}{\|\mathbf{h}_{1\mathrm{eff}}\|} \end{bmatrix}^T \mathbf{n}. \quad (10)$$

B. An Information Theoretic Analysis of ML and R-ML PIA Detection

The maximum achievable rate for a Bit-Interleaved Coded Modulation (BICM) equals the MI between transmitted and received signal vector, which in turn is a function of noise power and channel gains. There is no closed-form expression to compute MI for discrete alphabets; instead it can be approximated with Monte-Carlo simulations over a large number of channel N_H and noise N_n realizations. Instantaneous constrained BICM MI for optimum ML detection is defined by (11). For PIA detection, the instantaneous sum MI equals to

$$I_{\mathrm{PIA}} = \underbrace{I\left(X_0; \mathbf{Y}_{\mathrm{MF}}|\boldsymbol{\alpha}, \boldsymbol{\gamma}, M_0, M_1\right)}_{\text{MI for the first CW}} + \underbrace{I\left(X_1; \mathbf{Y}_{\mathrm{MF}}|\boldsymbol{\alpha}, \boldsymbol{\gamma}, M_0, M_1\right)}_{\text{MI for the second CW}}, \quad (14)$$

where $I\left(X_0; \mathbf{Y}_{\mathrm{MF}}|\boldsymbol{\alpha}, \boldsymbol{\gamma}, M_0, M_1\right)$ can be computed as (12) and $I\left(X_1; \mathbf{Y}_{\mathrm{MF}}|\boldsymbol{\alpha}, \boldsymbol{\gamma}, M_0, M_1\right)$ can be straightforwardly deduced from (12). PIA detection is a suboptimal solution for TM4; as it is shown in (13) applying MI chain rule, sum MI for two streams using SIC-IA detection equals to the MI of ML joint detection, and thus, to achieve optimum performance and complexity reduction, it is essential to set up the receiver into SIC detection mode. IF and MMSE receivers with corresponding per-stream SNR SNR_m^{IF} and SINR $SINR_m^{\mathrm{MMSE}}$

$$SNR_m^{\mathrm{IF}} = \frac{1}{N_0 n_{\mathrm{tx}}} \|\mathbf{h}_m\|^2, \quad (15)$$

$$SINR_m^{\mathrm{MMSE}} = \frac{1}{[(\mathbf{I}_{n_{tx}} + \frac{1}{N_0 n_{\mathrm{tx}}} \mathbf{H}^H \mathbf{H})^{-1}]_{mm}} - 1, \quad (16)$$

where $m = 1, 2$ is an index of the stream, are proven to upper and lower bound the performance of the ML-receiver [10], what is reflected in (13). Fig.1 supports the theoretical expectations: R-ML PIA receiver shows near-optimum performance in comparison with ML and is bounded by the performance of IF and MMSE $W_{\mathrm{MMSE}} = (\mathbf{H}^H \mathbf{H} + (\frac{1}{N_0 n_{\mathrm{tx}}})^{-1} \mathbf{I}_{n_{tx}})^{-1} \mathbf{H}^H$ receivers.

$$I\left(X;Y|SNR,M\right) = \log M - \frac{1}{MN_hN_n}\left(\sum_{x\in Q^M}\sum_c^{N_h}\sum_z^{N_n}\log\frac{\sum_{x\in Q^M}\exp(-SNR\,|y-hx'|^2)}{\exp(-|n|^2)}\right) \tag{20}$$
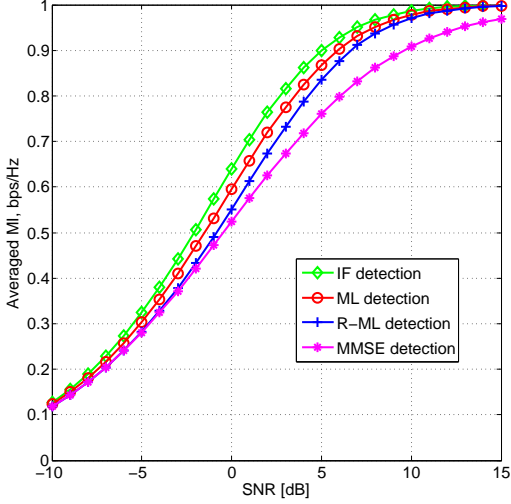
Fig. 1. Average Normalized Sum MI for two CWs belonging to QPSK for 8-tap Rayleigh channel for IF, ML, R-ML PIA and MMSE receivers

IV. PHY ABSTRACTION METHODOLOGY

Since we investigate R-ML PIA receiver, where detection is done on per-stream basis, the abstraction methodology can be considered symmetric per CW. PHY abstraction ultimately aims to predict BLER based on current channel state and noise power, thus, the input parameters of the abstraction model would be effective compensated channel gains $\boldsymbol{\alpha}$ and $\boldsymbol{\gamma}$ and noise power N_0. The MIESM methodology for each spatial stream m consists of the following steps:

1) Compute LQM per subcarrier k MI_k^m.
2) Obtain the single effective LQM MI_{eff}^m for each channel use.
3) Reversely map MI_{eff}^m to the $SINR_{\text{eff}}^m$.
4) Find the estimated BLER $BLER_{\text{eff}}^m$ corresponding to $SINR_{\text{eff}}^m$.
5) Calibrate results using the adjustment coefficients β_0^m and β_1^m.

Recall that the CW_0 with MCS^0 is decoded in presence of interfering CW_1 with MCS^1 and vice versa.

A. Obtaining LQM

Mapping process is the heart and the most challenging point of the abstraction methodology. Mapping can be done via direct computation of MI_k^m for each particular channel realization using (12), which would be very precise, but is time and CPU consuming. Instead of this, we propose to utilize from the precomputed LUT: channel statistics $||\boldsymbol{\alpha}_k||$, $||\boldsymbol{\gamma}_k||$, N_0 and corresponding MI_k, obtained using (12) by running Monte-Carlo simulations for a large number of channel realizations and noise variances, and then stored in LUT (17). The choice of building the LUT based on $||\boldsymbol{\alpha}_k||$, $||\boldsymbol{\gamma}_k||$ is motivated by the implementation complexity: after MI_k

estimates are obtained for each of the channel realization, it is necessary to build a gridded surface $\text{MI}_{\text{LUT}_k} = \text{F}(\boldsymbol{\alpha}_k, \boldsymbol{\gamma}_k, N_0)$, from the scattered data set with the help of data griding, interpolation and surface fitting tools, which is not trivial when $\boldsymbol{\alpha}_k$ and $\boldsymbol{\gamma}_k$ are two-dimensional complex vectors. It could be possible to separate phase and amplitude for each of the channel coefficients, but this would lead to an unfeasibly high dimensionality of the LUT. However, the drawback of the choice of $||\boldsymbol{\alpha}_k||$, $||\boldsymbol{\gamma}_k||$ consists the loss of the channel phase information, and the accuracy in terms of the Minimum Square Error (MSE) is compared with the direct computation method (11) for a few MCS values.

$$MI_{\text{LUT}_k}(||\boldsymbol{\alpha}_k||, ||\boldsymbol{\gamma}_k||, N_0, M_0, M_1) = I\left(X_0; \mathbf{Y}_{\text{MF}}\big|\boldsymbol{\alpha}_k, \boldsymbol{\gamma}_k, N_0, M_0, M_1\right). \tag{17}$$

For BICM, MI is limited by the modulation order M of a 2^M QAM constellation and saturates at different SNR or SINR values for different M. Thus, a library of LUTs is needed to take into account different combinations of modulation orders for both CWs. Per-subcarrier $MI_{\text{LUT}_k}^m$ is then averaged among the subcarriers and technically becomes an equivalent of MI in a single-state channel:

$$MI_{\text{eff}}^m = \frac{\sum_{k=1}^{K} MI_{\text{LUT}_k}^m(||\boldsymbol{\alpha}_k||, ||\boldsymbol{\gamma}_k||, N_0, M_0, M_1)}{\beta_0^m K}, \tag{18}$$

where β_0^m is the first adjustment factor to compensate for modulation and coding rate.

B. Obtaining Effective SNR

We are now looking for a direct relation between MI_{eff}^m and $SINR_{\text{eff}}^m$. We assume that there exists an equivalent one-tap Single-Input-Single-Output (SISO) channel with a signal model (19) and averaged MI (20):

$$\widetilde{y}_k = \widetilde{h}_k\widetilde{x}_k + \widetilde{n}_k, \tag{19}$$

where $\widetilde{x}_k \in Q^M$ is a received complex symbol with variance of $\widetilde{\sigma}^2$, Q^M is a modulation alphabet of order $M \in \{2, 4, 6\}$, $\widetilde{h}_k$ is flat fading Rayleigh SISO channel with i.i.d. ZMCSCG random variables with a variance of 0.5 per dimension and $\widetilde{n}_k$ is ZMCSCG noise of double-sided power spectral density $N_0/2$. Then a one-to-one mapping between MI_{eff}^m and $SINR_{\text{eff}}^m$ can be obtained by the means of linear interpolation of (20) for a known value of MI_{eff}^m. Here $M = M_m$, $SINR_{\text{eff}}^m = \beta_1^m SINR_{\text{eff}}^m$ and β_1^m is the second adjustment factor to compensate for modulation and coding rate.

C. Finding Estimated BLER

Assuming that effective SNR in a fading channel results in the same BLER as it would result in an AWGN channel,

$$BLER^m(\mathbf{H}_{\text{eff}}, N_0, \text{MCS}^m) \cong BLER_{\text{AWGN}}(\beta_1 SNR_{\text{eff}}, \text{MCS}^m). \tag{21}$$
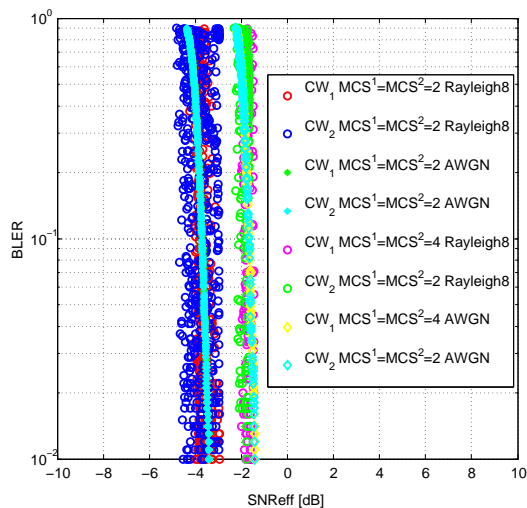
Fig. 2. Performance validation for CW_0 and CW_1 belonging to QPSK. Predicted BLER of TM4 for $MCS^0, MCS^1 = 2$ and $MCS^0, MCS^1 = 4$ in 8-tap Rayleigh channel.

Fig. 3. Performance validation for CW_0 and CW_1 belonging to 16QAM. Predicted BLER of TM4 for $MCS^0, MCS^1 = 10$ in 8-tap Rayleigh channel.

It is important that the AWGN curves are precomputed for the full range of MCS and correspond to TM4, since various amount of Resource Elements is used for different transmission modes, resulting in a rate-dependent shift of the AWGN curves.

D. PHY Abstraction Training

The calibration of the adjustment factors β_0^m and β_1^m is an important step of PHY abstraction validation. The detailed analysis of the calibrating approaches has been done in [17]; the best fitting results are shown using logarithmic scale. Minimum Square Error (MSE) between $SINR_{\text{eff}}^m$ and $SINR_{\text{AWGN}}^m$ is an adequate criteria for the training:

$$\beta_{\text{opt}_0}^m, \beta_{\text{opt}_1}^m = \underset{\beta_0^m, \beta_1^m}{\arg \min} \frac{1}{N_H N_n} \left[\sum_c^{N_H} \sum_z^{N_n} |SINR_{\text{eff}}^m(\beta_0^m, \beta_1^m, MCS^m) - SINR_{\text{AWGN}}^m(MCS^m)|^2 \right].$$

(22)

V. RESULTS

The simulations were carried out using the downlink simulator of OpenAirInterface (OAI) – an open source LTE platform developed at EURECOM [1] with respect to 3GPP standards [18], [19], [20] with a high degree of realism and flexibility. The important part of the simulations was the careful generation of the input link level data for AWGN and frequency-selective channels. For the AWGN simulation, the channel was generated with the help of the spatial correlation matrix, that nullifies cross-layer interference, and 10000 packets were transmitted with the perfect Channel Estimation (CE) at the UE. For the frequency-selective simulation, 8-tap Rayleigh fading channel with i.i.d. entries and the delay spread of 0.8 microseconds was chosen, and 1000 packets were transmitted over 100 channel realizations for the wide range of noise variances targeting BLER of 10^{-2} applying

perfect CE at the receiver as well. These traces were then used to obtain the calibration coefficients that are stored for each MCS and can be used for any random channel realization with the accuracy provided in Table I. The abstraction results for CWs coming from QPSK constellation (Fig. 2), 16QAM (Fig. 3) and a combination of these two constellations (Fig. 4) should be read as follows: the closer the Rayleigh curves (plotted in circles) are to the corresponding AWGN curve (plotted in diamonds), the more accurate is the abstraction. The calibration precision of LUT method for QPSK constellation is verified with the direct MIESM mapping at the stage of obtaining LQM per subcarrier.
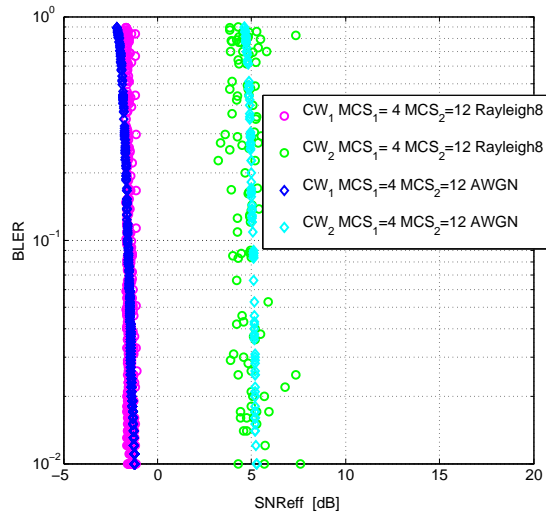
Fig. 4. Performance validation for CW_0 and CW_1 belonging to QPSK and 16QAM respectively. Predicted BLER of TM4 for $MCS^0 = 4$ and $MCS^1 = 12$ in 8-tap Rayleigh channel

From a comparative analysis of Table I and Table II, it is clear that we have a good match between these two methods, and thus, the LUT based MIESM PHY abstraction can be considered as introducing sufficient accuracy in terms of MSE,

TABLE I
CALIBRATION RESULTS FOR MIESM LUT ABSTRACTION METHODOLOGY
IN 8-TAP RAYLEIGH CHANNEL

MCS^0	MCS^1	MSE^0_{LUT}	MSE^1_{LUT}	$\beta^0_{LUTopt_0}$	$\beta^1_{LUTopt_0}$	$\beta^0_{LUTopt_1}$	$\beta^1_{LUTopt_1}$
2	2	0.0334	0.0544	15.7701	24.0338	0.2292	0.2107
4	4	0.0253	0.0403	8.1128	19.8789	0.1415	0.1067
4	12	0.0369	0.6021	11.2565	0.7811	0.1177	0.6284
10	10	0.3781	0.5707	0.6762	0.6772	0.4860	0.4315
12	12	0.7480	0.8817	0.7734	0.8343	0.6070	0.6023

TABLE II
CALIBRATION RESULTS FOR DIRECT MIESM MAPPING ABSTRACTION
METHODOLOGY FOR QPSK IN 8-TAP RAYLEIGH CHANNEL

MCS^0	MCS^1	MSE^0_{direct}	MSE^1_{direct}	$\beta^0_{directopt_0}$	$\beta^1_{directopt_0}$	$\beta^0_{directopt_1}$	$\beta^1_{directopt_1}$
2	2	0.0364	0.0409	8.2438	4.9157	0.2300	0.2731
4	4	0.0217	0.0300	2.4298	2.3646	0.1839	0.1870

despite the loss of channel phase information. However, it could be surprising that the CWs with identical MCS require different calibration coefficients. In fact, the two streams given the same MCS show the exact same performance in AWGN channel due to interference absence provided by the spatial correlation matrix, while in frequency selective channel, the CW_0 always enjoys higher MI due to precoder selection strategy, and shows better performance (3dB), which leads to non-equal adjusting coefficients for both streams.

VI. CONCLUSION

We have developed and validated link abstraction methodology for the the parallel interference aware MIMO receiver, where the two codewords are coming from QPSK, 16 QAM and combination of these two constellations. Our methodology is based on precomputed LUT library of MI values for R-ML PIA detection. The LUT is based on the norms of the columns of the channel matrix H_{eff} and noise variance N_0. The results of LUT-based abstraction are shown to be accurate enough and this methodology can be easily deployed in performance prediction devices as well as system level simulators. We also performed a comparison between the accuracy achieved by the LUT-based MIESM method with direct MIESM mapping and found that the loss of channel phase information does not introduce a significant degradation in the performance. In future work we are planning to extend the proposed abstraction methodology to a successive interference cancellation (SIC) receiver, which is the optimal detection strategy for transmission mode 4 with two codewords. Moreover, the suboptimal precoder selection strategy used in this paper for PIA detection, would also turn into optimum for the SIC case and thus the abstraction methodology used in this paper will become more accurate as well. In addition, we plan to extend the simulations to other frequency-selective channel models such as the 3GPP Spatial Channel Model (SCM), that may introduce a significant difference in the calibration coefficients.

VII. ACKNOWLEDGMENT

REFERENCES

[1] B. R. Bilel, N. Navid, K. Raymond, and B. Christian, "Openair-interface large-scale wireless emulation platform and methodology," in *In PM2HW2N 6th ACM International Workshop on Performance Monitoring, Measurement and Evaluation of Heterogeneous Wireless and Wired Networks*, 2011, pp. 109–112.

[2] I. Latif, F. Kaltenberger, N. Nikaein, and R. Knopp, "Large scale system evaluations using PHY abstraction for LTE with openairinterface," in *Proceedings of the 6th International ICST Conference on Simulation Tools and Techniques*. ICST (Institute for Computer Sciences, Social-Informatics and Telecommunications Engineering), 2013, pp. 24–30.

[3] E. Tuomaala and H. Wang, "Effective SINR approach of link to system mapping in OFDM/multi-carrier mobile network," in *Mobile Technology, Applications and Systems, 2005 2nd International Conference on*, Nov 2005.

[4] X. Lei and Z. Jin-bao, "An accurate mean mutual information computational approach of link performance abstraction," in *Signal Processing (ICSP), 2010 IEEE 10th International Conference on*, Oct 2010, pp. 1552–1556.

[5] IEEE, " 802.16m Evaluation Methodology Document (EMD)," Jan 2009.

[6] K. Sayana, J. Zhuang, and K. Stewart, "Link performance abstraction based on mean mutual information per bit (MMIB) of the LLR channel," *IEEE 802.16 Broadband Wireless Access Working Group*, 2007.

[7] Z. Hanzaz and H. Schotten, "Analysis of effective SINR mapping models for MIMO OFDM in LTE system," in *Wireless Communications and Mobile Computing Conference (IWCMC), 2013 9th International*, July 2013, pp. 1509–1515.

[8] E. Stancanelli, F. Cavalcanti, and Y. Silva, "Revisiting the effective SINR mapping interface for link and system level simulations of wireless communication systems," in *Communications (LATINCOM), 2011 IEEE Latin-American Conference on*, Oct 2011, pp. 1–6.

[9] I. Latif, F. Kaltenberger, and R. Knopp, "Link abstraction for multiuser MIMO in LTE using interference-aware receiver," in *Wireless Communications and Networking Conference (WCNC), 2012 IEEE*, April 2012, pp. 842–846.

[10] S.-H. Moon, K.-J. Lee, J. Kim, and I. Lee, "Link performance estimation techniques for MIMO-OFDM systems with maximum likelihood receiver," *Wireless Communications, IEEE Transactions on*, vol. 11, no. 5, pp. 1808–1816, 2012.

[11] H. Lee, J. Lim, W. Park, and T. Kim, "Link performance abstraction for interference-aware communications (IAC)," in *Vehicular Technology Conference (VTC Fall), 2014 IEEE 80th*. IEEE, 2014, pp. 1–5.

[12] R. Ramesh, H. Koorapaty, J.-F. Cheng, and K. Balachandran, "A physical layer abstraction for maximum likelihood demodulation of MIMO signals," in *Vehicular Technology Conference, 2009. VTC Spring 2009. IEEE 69th*, April 2009, pp. 1–5.

[13] 3GPP, "Network-assisted interference cancellation and suppression for LTE," 3GPP, Tech. Rep. TR 36.866 v12.0.1, March 2014.

[14] E. Akay and E. Ayanoglu, "Low complexity decoding of bit-interleaved coded modulation for M-ary QAM," in *Communications, 2004 IEEE International Conference on*, vol. 2, June 2004, pp. 901–905 Vol.2.

[15] R. Ghaffar and R. Knopp, "Low complexity metrics for BICM SISO and MIMO systems," in *Vehicular Technology Conference (VTC 2010-Spring), 2010 IEEE 71st*, May 2010, pp. 1–6.

[16] J. Lee, D. Toumpakaris, and W. Yu, "Interference mitigation via joint detection," *Selected Areas in Communications, IEEE Journal on*, vol. 29, no. 6, pp. 1172–1184, June 2011.

[17] K. Brueninghaus, D. Astély, T. Salzer, S. Visuri, A. Alexiou, S. Karger, and G.-A. Seraji, "Link performance models for system level simulations of broadband radio access systems," in *in Proceedings IEEE International Symposium PIMRC*, vol. 4, 2005, pp. 2306–2311.

[18] 3GPP, "Evolved universal terrestrial radio access (E-UTRA); physical layer procedures," 3GPP, Tech. Rep. Technical Specification 36.213–V12.3, Oct 2014.

[19] ——, "Evolved universal terrestrial radio access (E-UTRA); physical channels and modulation," 3GPP, Tech. Rep. Technical Specification 36.211–V12.6.0, July 2015.

[20] ——, "Evolved universal terrestrial radio access (E-TRA); multiplexing and channel coding," 3GPP, Tech. Rep. Technical Specification 36.212–V12.7.0, July 2015.